

Use of geospatial data and fuzzy algebraic operators to landslide-hazard mapping

Biswajeet Pradhan · Saro Lee ·
Manfred F. Buchroithner

Received: 15 October 2008 / Accepted: 5 March 2009 / Published online: 1 April 2009
© Società Italiana di Fotogrammetria e Topografia (SIFET) 2009

Abstract Geospatial data base creation for landslide-hazard mapping is often an almost inhibitive activity. This has been the reason that for quite some time landslide-hazard analysis was modeled on the basis of spatially related factors. This paper presents the use of fuzzy logic to landslide-hazard analysis in the Penang Island, Malaysia, using remote sensing data and a geographic information system (GIS). To achieve the goal, a data-derived model (frequency ratio) and a knowledge-derived model (fuzzy operator) were combined for landslide-hazard analysis. Landslide locations within the study areas were identified by interpreting aerial photographs, satellite images and field surveys. The nine factors that influence landslide occurrence were extracted from the database and the frequency ratio coefficient for each factor was computed. Using the factors and the identified landslide, the fuzzy membership values were calculated. Then fuzzy algebraic operators were applied to the fuzzy membership values for landslide-hazard mapping. Finally, the produced map was verified by comparing with existing landslide locations for calculating prediction accuracy. Among the fuzzy operators, in the case in which the gamma operator ($\lambda=0.8$) showed the best

accuracy (80%) while the case in which the fuzzy or operator was applied showed the worst accuracy (56%).

Keywords Landslide · Hazard · GIS · Fuzzy operator · Fuzzy membership · Frequency ratio · Malaysia

Introduction

Landslides are major natural geological hazards and, each year, is responsible for enormous property damage and both direct and indirect costs. Malaysia experiences frequent landslides, with the most recent occurring in 2000, 2001, 2004, 2007, and 2008. They often result in significant damage to people and property. In Penang Island, much damage was caused by the torrential rainfall causing landslides and mudslides, and, because there was little effort to assess or predict the event, damage was extensive. Through scientific analysis of landslides, we can assess and predict landslide-hazardous areas and, by allowing proper preparation, decrease landslide damage. In order to achieve this, landslide-hazard analysis techniques were cross-applied and verified using a fuzzy membership model.

There have been many studies carried out on landslide-hazard evaluation using GIS; for example, Guzzetti et al. (1999) summarized many landslide-hazard evaluation studies. Recently, there have been studies on landslide-hazard evaluation using GIS, and many of these studies have applied probabilistic models (Akgun et al. 2007; Dahal et al. 2007; Clerici et al. 2006; Cevik and Topal 2003; Rowbotham and Dudycha 1998; Jibson et al. 2000; Luzi et al. 2000; Parise and Jibson 2000; Baeza and Corominas 2001; Clerici et al. 2002; Donati and Turrini 2002; Zhou et al. 2002; Lee et al. 2004b). One of the statistical models available, the logistic regression models, has also been

B. Pradhan (✉)
Institute of Cartography, Dresden University of Technology,
01062 Dresden, Germany
e-mail: Biswajeet.Pradhan@mailbox.tu-dresden.de

S. Lee
Geoscience Information Center, Korea Institute of Geoscience
and Mineral Resources (KIGAM) 30,
Kajung-Dong, Yusung-Gu,
Daejeon, Korea

M. F. Buchroithner
Faculty of Forestry, Geo and Hydro-Science,
Dresden University of Technology,
01062 Dresden, Germany

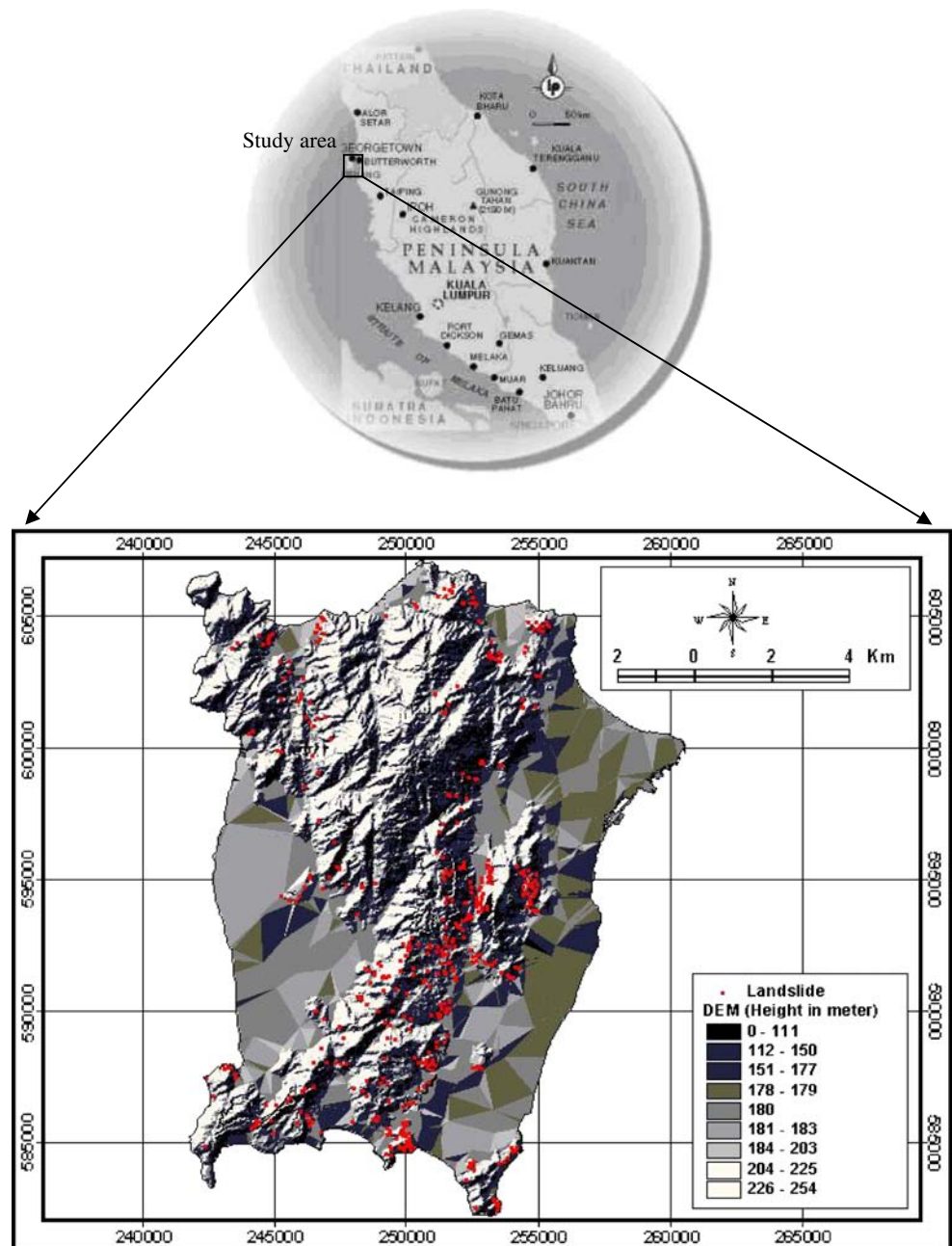
applied to landslide-hazard mapping (Tunusluoglu et al. 2007; Lamelas et al. 2008; Wang and Sassa 2005; Süzen and Doyuran 2004; Dai and Lee 2002; Ohlmacher and Davis 2003; Mansor et al. 2007; Pradhan et al. 2006, 2008), as has the geotechnical model and the safety factor model (Gokceoglu et al. 2000; Romeo 2000; Refice and Capolongo 2002; Carro et al. 2003; Shou and Wang 2003; Zhou et al. 2003, Lee 2007, Lee and Pradhan 2007). As a new approach to landslide-hazard evaluation using GIS, data mining, safety factor, fuzzy logic and artificial neural network models have been applied (Gomez and Kavzoglu, 2005; Xie et al. 2004; Ercanoglu and Gokceoglu 2002; Pistocchi et al. 2002; Lee et

al. 2003a, b, 2004a; Tangestani 2004; Lee and Pradhan 2006; Pradhan and Lee 2007, 2008 ; Catani et al. 2005).

Study area

Penang Island, which has suffered much landslide damage following heavy rains, was selected as a suitable pilot area to evaluate landslide-hazard analysis using the fuzzy operator model (Fig. 1). Penang is one of the 13 states of the Federal Territory of Malaysia and is located on the Northwest coast of the Malaysia peninsula. It is bounded to

Fig. 1 The study area with landslide locations



north and east by the state of Kedah, to south by the state of Perak, and to west by the Straits of Malacca and Sumatra (Indonesia). Penang consists of the island of Penang, and a coastal strip on the mainland, known as Province Wellesley. The island covers an area of 285 km², and is separated from the mainland by a channel. The study area is located approximately between latitudes 5°15' N to 5°30' N and longitudes 100°10'E to 100°20'E. The land-use in the study area is mainly peat swamp forest, plantation forest, inland forest, scrub, grassland, and ex-mining area. The slope of the area ranges from 25° to as much as 87°. The relief of the study area varies from 0–420 m above mean sea level. Based on the Malaysian Meteorological Department, the temperature of the northern part of Penang ranges between 29°C and 32°C and mean relative humidity varies between 65% and 70%. The highest temperature is during April to June while the relative humidity is lowest in June, July and September. The rainfall of about 58.6 mm to 240 mm per month is recorded in the study area (at the Bayan Lepas weather station provided by the Malaysian Meteorological Services Department). GPS data for landslide locations has been collected for various parts of Penang Island in the month of July and October 2006. There were about 21 active landslides recorded from the field survey and these were used to verify the model output.

Spatial database creation

To apply the fuzzy approach model, a spatial database that considers landslide-related factors was designed and constructed. These data are available in Malaysia either

as paper or as digital maps. The spatial database constructed is listed in Table 1. Landslide occurrence areas were detected in the Penang area, Malaysia by interpretation of aerial photographs and field surveys. A landslide map was prepared from aerial photographs, in combination with the GIS, and this was used to evaluate the frequency and distribution of shallow landslides in the area. These landslides were detected from aerial photographs by interpreting breaks in the forest canopy, bare soil, and other typical geomorphic characteristics of landslide scars. A total of 463 landslides were mapped within 285 km² to assemble a database to assess the number of landslides in the study area. The inventory map was prepared by a structural geologist with a profound knowledge on aerial photo interpretation. These landslides were vectorized from the aerial photographs and the location of the scar extent was transformed into a grid database with 10×10-m cell size. Topography and lithology databases were constructed and lineament, land cover and vegetation index value extracted from Landsat TM satellite image for the analysis. Then, the calculated and extracted factors were converted to a 10 m×10 m grid (ARC/INFO GRID type). The lineament and land cover were detected from satellite images such as Landsat TM (Thematic Mapper) images. There were ten landslide-inducing factors considered in calculating the fuzzy membership function. These factors were transformed into a vector-type spatial database using the GIS. For the DEM creation, 10-m interval contours and survey base points showing the elevation values were extracted from the 1:25,000-scale topographic maps and triangulated irregular network (TIN) was made using the

Table 1 Thematic data layer of study area

Classification		GIS data type		Scale or resolution	
Spatial database	Factor	Spatial database	Factor	Spatial database	Factor
Landslide	Landslide	ARC/INFO Polygon coverage	ARC/INFOGRID	1:25,000	10 m×10 m
Topographic Map	Slope Aspect Curvature	ARC/INFO Line and Point Coverage		1:25,000	
Drainage Map	Distance from drainage	ARC/INFO Line Coverage			
Soil Map	Types	ARC/INFO Polygon coverage		1:100,000	
Geology Map	Litho types Distance from lineaments	ARC/INFO Polygon, Line coverage		1:63,300	
Land Cover	Land Cover	ARC/INFO GRID		30 m×30 m	
NDVI	NDVI	ARC/INFO GRID		10 m×10 m	
Precipitation	Precipitation	GRID		10 m×10 m	

elevation value. A DEM (digital elevation model) was made using the inverse distance weighting (IDW) interpolation method with 10 m resolution. Using this DEM, slope angle, slope aspect, and slope curvature were calculated. In the present study, substantial attention has been given for slope conditions. Slope configuration and steepness plays an important role in conjunction with lithology. Maps have been produced showing slope steepness; the slope varies from 0 to 45° in plain areas to near-vertical cliffs to greater than 45° in the steep areas. In the case of the aspect map, there are eight directions shown for the different direction of slope. In the case of the curvature, negative curvatures represent concave, zero curvature represent flat and positive curvatures represents convex. The curvature map was prepared using the avenue routine in ArcView 3.2. In addition, the distance from drainage was calculated using the topographic database. The drainage buffer was calculated at 100-m intervals and classified into ten equal area classes. The lithology map is prepared from a 1:63,300-scale geological map. A structural geologist interpreted the Spot 5 image by photo interpretation and detected the lineaments and the distance from lineament is calculated based on the Euclidean distance method in ArcView 3.2. The lineament buffer was calculated in 100-m intervals and classified into ten equal area classes. Land-use map was prepared using Landsat TM image (30 m spatial resolution) using unsupervised classification (ISODATA) method and field survey. There were 11 land-use classes identified, such as urban, water, forest, agriculture, and barren area. Finally, the normalized difference vegetation index (NDVI) map was generated from SPOT 5 (2.5 m spatial resolution) satellite images. The NDVI value was calculated using the formula $NDVI = (IR - R)/(IR + R)$, where IR is the energy reflected in the infrared portion of the electromagnetic spectrum, and R is the energy reflected in the red portion of the electromagnetic spectrum. The NDVI is useful in delineating vegetation. The soil map was obtained from existing hard copy soil map (1:100,000) from Department of Soil, Malaysia and is the only existing soil map for the study area. There are about 14 types of different soil series identified and used in the analysis. The precipitation map was prepared using the last 20 years of historical rainfall data. In the study area, there are only two rain-gauge stations located. So, data used in this study is collected from these stations and a statistical distribution of the accumulated average precipitation was prepared in GIS.

Using the factors and the detected landslide, the relationships were calculated using the frequency ratio, one of the probabilistic models. Then, the fuzzy membership values were also calculated using the frequency ratio. The fuzzy membership values were combined using the fuzzy and, fuzzy

or, fuzzy algebraic product, fuzzy algebraic sum, and fuzzy gamma operators (13 cases) for landslide-hazard mapping. Finally, the map was verified by comparing with existing landslide locations for calculating prediction accuracy.

Fuzzy operator model was applied using the database and landslide-hazard map was created. Finally, the map was verified and compared using known landslide locations for quantitative verification. In the study, Geographic Information System (GIS) software, ArcView 3.2, and ArcGIS 9.0 version software packages were used as the basic analysis tools for spatial management and data manipulation. Overall, the Penang data set comprised 2,493 rows by 1,887 columns, for a total cell number of 4,704,291. Landslides had occurred in 463 of these cells.

Methodology

The fuzzy set theory introduced by Zadeh (1965) is one of the tools used to handle the complex problems. Therefore, the fuzzy set theory has been commonly used for many scientific studies in different disciplines. The idea of fuzzy logic is to consider the spatial objects on a map as members of a set. In the classical set theory, an object is a member of a set if it has a membership value of 1, or is not a member if it has a membership value of 0. In the fuzzy set theory, membership can take on any value between 0 and 1 reflecting the degree of certainty of membership. The fuzzy set theory employs the idea of a membership function that expresses the degree of membership with respect to some attribute of interest.

With maps, generally, the attribute of interest is measured over discrete intervals, and the membership function can be expressed as a table relating map classes to membership values. Fuzzy logic is attractive because it is straightforward to understand and implement. It can be used with data from any measurement scale and the weighing of evidence is controlled entirely by the expert. The fuzzy logic method allows for more flexible combinations of weighted maps, and could be readily implemented with a GIS modeling language. This is different from data-driven approaches such as weights of evidence or logistic regression, which use the locations of known objects such as landslides to estimate weights or coefficients. The idea of using fuzzy logic in landslide-hazard mapping is to consider the spatial objects on a map as members of a set. For example, the spatial objects could be areas on an evidence map and the set defined as 'areas hazardous to landslide'. Fuzzy membership values must lie in the range (0, 1), but there are no practical constraints on the choice of the fuzzy membership values. Values are chosen to reflect the degree of membership of a set, based on subjective judgment. Given two or more maps with fuzzy membership functions for the same set, a variety

of operators can be employed to combine the membership values.

Zimmerman (1996) discussed a variety of combination rules. Bonham-Carter (1994) discussed five operators, namely the fuzzy and, fuzzy or, fuzzy algebraic product, fuzzy algebraic sum, and fuzzy gamma operator. This study uses the five fuzzy operators for combining the fuzzy membership functions.

The fuzzy and is equivalent to a Boolean AND (logical intersection) operation on classical set values of (1). It is defined as:

$$\mu_{\text{combination}} = \text{MIN}(\mu_A, \mu_B, \mu_C, \dots), \tag{1}$$

where $\mu_{\text{combination}}$ is the calculated fuzzy membership function, μ_A is the membership value for map A at a particular location and μ_B is the value for map B, and so on.

The fuzzy or is like the Boolean OR (logical union in that the output membership values are controlled by the maximum values of any of the input maps. The fuzzy or is defined as:

$$\mu_{\text{combination}} = \text{MAX}(\mu_A, \mu_B, \mu_C, \dots). \tag{2}$$

The fuzzy algebraic product is defined as:

$$\mu_{\text{combination}} = \prod_{i=1}^n \mu_i, \tag{3}$$

where μ_i is the fuzzy membership function for the i -th map, and $i=1, 2, \dots, n$ maps are to be combined.

The fuzzy algebraic sum is complementary to the fuzzy algebraic product, being defined as:

$$\mu_{\text{combination}} = 1 - \prod_{i=1}^n (1 - \mu_i). \tag{4}$$

The gamma operation is defined in terms of the fuzzy algebraic product and the fuzzy algebraic sum by:

$$\mu_{\text{combination}} = (\text{Fuzzy algebraic sum})^{\lambda} * (\text{Fuzzy algebraic product})^{1-\lambda}, \tag{5}$$

where λ is a parameter chosen in the range (0,1), and the fuzzy algebraic sum and fuzzy algebraic product are calculated using Eqs. 3 and 4, respectively. In the fuzzy gamma operation, when λ is 1, the combination is the same as the fuzzy algebraic sum, and when λ is 0 the combination equals the fuzzy algebraic product. Judicious choice of λ produces output values that ensure a flexible compromise between the ‘increase’ tendencies of the fuzzy algebraic sum and the ‘decrease’ effects of the fuzzy algebraic product.

Like the membership function, the frequency ratio was calculated. The frequency ratio is shown in Table 2 for all factors. The spatial relationships between the land-

slide location and each landslide-related factor were analyzed by using the probability model–frequency ratio. The frequency ratio, a ratio between the occurrence and absence of landslides in each cell, was calculated for each factor’s type or range that had been identified as significant with respect to causing landslides. An area ratio for each factor’s type or range to the total area was calculated. Finally, frequency ratios for each factor’s type or range were calculated by dividing the landslide occurrence ratio by the area ratio. If the ratio is greater than 1, the relationship between landslides and the factors is higher and, if the ratio is less than 1, the relationship between landslide and each factor’s type or range is lower. Then, the frequency ratio was normalized between 0.00 and 1.00 to create the fuzzy membership value.

Application of fuzzy logic to landslide-hazard mapping

The input factors were combined for assigning membership functions. Nine landslide causal factors (slope, aspect, curvature, distance from drainage, soil, distance from lineament, NDVI, precipitation, and land cover) were combined to generate the final hazard map using fuzzy operators such as fuzzy and, fuzzy or, fuzzy algebraic product, fuzzy algebraic sum, and fuzzy gamma operator. In the case of fuzzy gamma operator, the value of λ was set to 0.025, 0.05, 0.1, 0.2, 0.3, 0.4, 0.5, 0.6, 0.7, 0.8, 0.9, 0.95, and 0.975 to detect its effect on the landslide-hazard map.

Using the fuzzy membership function (Table 2) and the fuzzy operator (from Eqs. 1 to 5), the landslide-hazard index (LHI) values were computed for the 17 cases including the 13 cases in which the gamma operator was used. The computed LHI values were mapped to allow interpretation such as that illustrated for example in Fig. 2. The values were classified into equal areas and grouped into five classes for visual interpretation. For example, in the case of applying the fuzzy and product, the minimum, mean, maximum and standard deviation values of each LHI are 0.00, 0.112, 0.3281, and 0.0254, respectively. In the case of applying the fuzzy algebraic sum, the minimum, mean, maximum, and standard deviation values of each LHI are 0.0042, 0.0277, 0.0513, and 0.0078, respectively. In the case of applying the gamma operator ($\lambda=0.975$), the minimum, mean, maximum, and standard deviation values of each LHI are 0.000, 0.3003, 1.7448, and 0.5046, respectively. Also, in the case of applying the gamma operator ($\lambda=0.8$), the minimum, mean, maximum, and standard deviation values of each LHI are 0.000, 0.0061, 0.00092, and 0.00117, respectively.

Table 2 Spatial relationships between each factor and landslide and fuzzy membership values

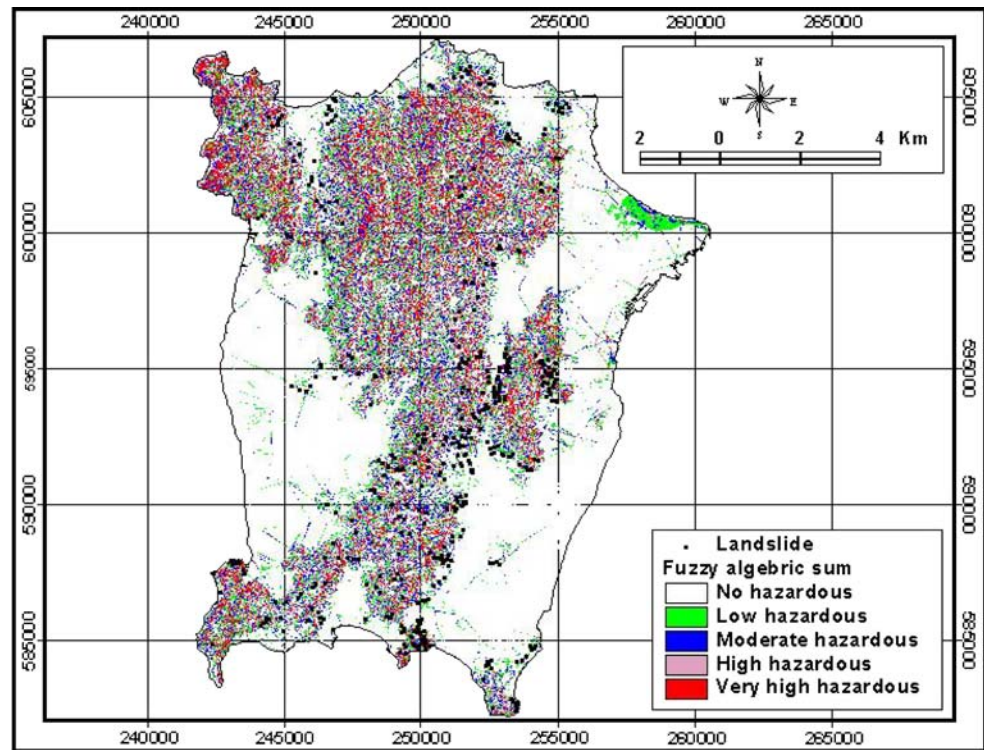
Factor	Class	Landslide occurrence Points	Landslide occurrence Points %	Pixels in domain	Pixel %	Frequency ratio	Fuzzy membership function
Slope	0~5°	981098	33.20	0	0.00	0.00	0.00
	6~10°	276054	9.34	0	0.00	0.00	0.00
	11~15°	234326	7.93	21	4.54	0.57	0.11
	16~20°	218322	7.39	32	6.91	0.94	0.18
	21~25°	266234	9.01	43	9.29	1.03	0.19
	26~30°	221465	7.50	50	10.80	1.44	0.27
	31~35°	212850	7.20	30	6.48	0.90	0.17
	36~40°	230109	7.79	83	17.93	2.30	0.44
	41~45°	173227	5.86	87	18.79	3.21	0.61
Aspect	46~90°	141097	4.78	117	25.27	5.29	1.00
	Flat	1199400	40.59	13	2.80	0.07	0.00
	North	206629	6.99	41	8.85	1.27	0.56
	Northeast	207860	7.03	51	11.01	1.57	0.70
	East	228674	7.74	60	12.95	1.67	0.75
	Southeast	236988	8.02	82	17.71	2.21	1.00
	South	205108	6.94	58	12.53	1.80	0.81
	Southwest	206970	7.01	52	11.23	1.60	0.72
	West	228117	7.72	54	11.66	1.51	0.67
Curvature	Northwest	235036	7.95	52	11.23	1.41	0.63
	Concave	770757	26.09	50	10.80	0.41	0.07
	Flat	1419529	48.04	45	9.72	0.20	0.00
Distance from drainage	Convex	764496	25.87	368	79.48	3.07	1.00
	0~14 m	325460	11.01	21	4.54	0.41	0.00
	20~36 m	347537	11.76	43	9.29	0.79	0.42
	40~56 m	298382	10.10	61	13.17	1.30	1.00
	58~76 m	285453	9.66	58	12.53	1.30	0.99
	78~100 m	310971	10.52	48	10.37	0.99	0.64
	101~130 m	296818	10.05	52	11.23	1.12	0.79
	131~169 m	273396	9.25	48	10.37	1.12	0.79
	170~222 m	275609	9.33	49	10.58	1.13	0.81
Geology	223~331 m	272270	9.21	55	11.88	1.29	0.98
	332~2,064 m	268886	9.10	28	6.05	0.66	0.28
	Micro granite	43801	1.52	7	1.512	0.98	0.75
Soil	Alluvium	668834	23.34	2	0.432	0.01	0.00
	Granite	2151905	75.12	454	98.056	1.305	1.00
	Rengam-bukit temiang association	289450	10.03	96	20.73	2.07	1.00
	Selangor-kangkong association	34197	1.18	0	0.00	0.00	0.00
	Local alluvium-colluvium associ.	373655	12.94	13	2.81	0.22	0.10
	Serong series	80436	2.79	0	0.00	0.00	0.00
	Steep land	1506818	52.20	341	73.65	1.41	0.68
	Kuala kedah - permatang associ.	187057	6.48	0	0.00	0.00	0.00
	Urban land	413813	14.33	13	2.81	0.20	0.09
Distance from lineament	Rengam	1329	0.05	0	0.00	0.00	0.00
	0~89 m	297410	10.07	45	9.72	0.97	0.60
	90~180 m	307232	10.40	48	10.37	1.00	0.62
	181~275 m	293932	9.95	62	13.39	1.35	0.84

Table 2 (continued)

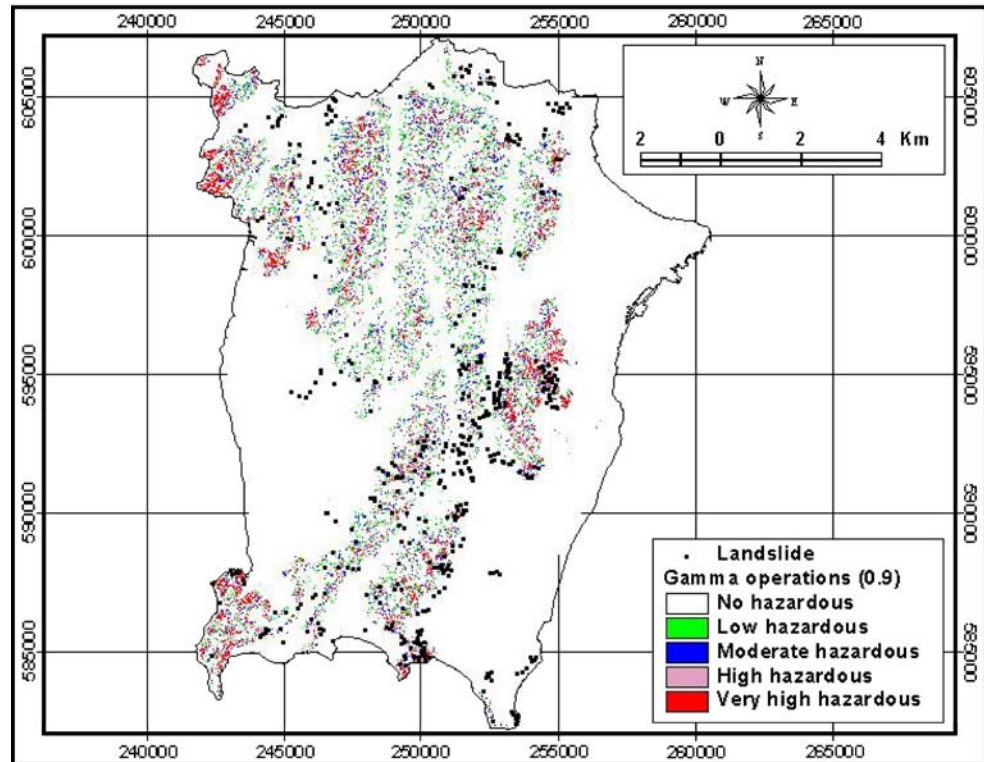
Factor	Class	Landslide occurrence Points	Landslide occurrence Points %	Pixels in domain	Pixel %	Frequency ratio	Fuzzy membership function
Land cover	276~377 m	294078	9.95	63	13.61	1.37	0.85
	378~494 m	294927	9.98	54	11.66	1.17	0.73
	495~640 m	294365	9.96	54	11.66	1.17	0.73
	641~841 m	294059	9.95	74	15.98	1.61	1.00
	842~1,150 m	292980	9.92	50	10.80	1.09	0.68
	1,151~1,777 m	293193	9.92	13	2.81	0.28	0.18
	1,778~5,317 m	292606	9.90	0	0.00	0.00	0.00
	Rubber	674705	22.05	53	11.50	0.52	0.03
	Clear land	75814	2.48	4	0.87	0.35	0.02
	Grass	256259	8.37	14	3.04	0.36	0.02
	Wood_BR	27618	0.90	4	0.87	0.96	0.05
	Coconut	88328	2.89	2	0.43	0.15	0.01
	Cultivated	774	0.03	1	0.22	8.58	0.48
	Wet padi	92852	3.03	0	0.00	0.00	0.00
	Belukar	12822	0.42	1	0.22	0.52	0.03
	Mangrove	144562	4.72	13	2.82	0.60	0.03
	Pri_forest	1067028	34.87	347	75.27	2.16	0.12
	Sand	22055	0.72	0	0.00	0.00	0.00
	Rock	10256	0.34	0	0.00	0.00	0.00
	Mud	83740	2.74	0	0.00	0.00	0.00
	Forest	498411	16.29	17	3.69	0.23	0.01
Tin mine	1876	0.06	5	1.08	17.69	1.00	
Nipah	2960	0.10	0	0.00	0.00	0.00	
Tin_mine	292	0.01	0	0.00	0.00	0.00	
Lake	63	0.00	0	0.00	0.00	0.00	
NDVI	-73 to -18	291092	10.05	33	7.13	0.71	0.06
	-17~1	300254	10.37	31	6.70	0.65	0.00
	2~21	297248	10.26	47	10.15	0.99	0.36
	22~32	315879	10.91	48	10.37	0.95	0.32
	33~37	358384	12.37	44	9.50	0.77	0.12
	38~40	322673	11.14	61	13.17	1.18	0.56
	41~43	373180	12.89	57	12.31	0.96	0.32
	44~45	226395	7.82	54	11.66	1.49	0.89
46~48	242836	8.38	45	9.72	1.16	0.54	
49~61	168249	5.81	43	9.29	1.60	1.00	
Precipitation	2,613~2,651 mm	297147	10.06	40	8.64	0.86	0.40
	2,652~1,676 mm	297745	10.08	45	9.72	0.96	0.47
	2,677~2,695 mm	301761	10.21	30	6.48	0.63	0.27
	2,696~2,707 mm	296883	10.05	40	8.64	0.86	0.40
	2,708~2,718 mm	293589	9.94	76	16.41	1.65	0.86
	2,719~2,730 mm	297716	10.08	40	8.64	0.86	0.40
	2,731~2,742 mm	313761	10.62	93	20.09	1.89	1.00
	2,743~2,753 mm	290201	9.82	63	13.61	1.39	0.71
2,754~2,763 mm	283131	9.58	29	6.26	0.65	0.29	
2,764~2,772 mm	282848	9.57	7	1.51	0.16	0.00	

Domain pixels in study area, *Domain (%)* (domain/total pixels in study area)×100, *landslide number* of landslide occurrences, *Landslide (%)* (landslide/total number of landslide occurrences)×100, *Frequency ratio* landslide (%)/domain (%), *fuzzy membership values* normalized value of the frequency ratio

Fig. 2 Landslide susceptibility maps using various fuzzy operators. **a** Application of fuzzy algebraic “sum” operator. **b** Application of fuzzy algebraic “and” operator. **c** Application of fuzzy gamma ($\lambda=0.8$) operator. **d** Application of fuzzy gamma ($\lambda=0.9$) operator. **e** Application of fuzzy gamma ($\lambda=0.975$) operator

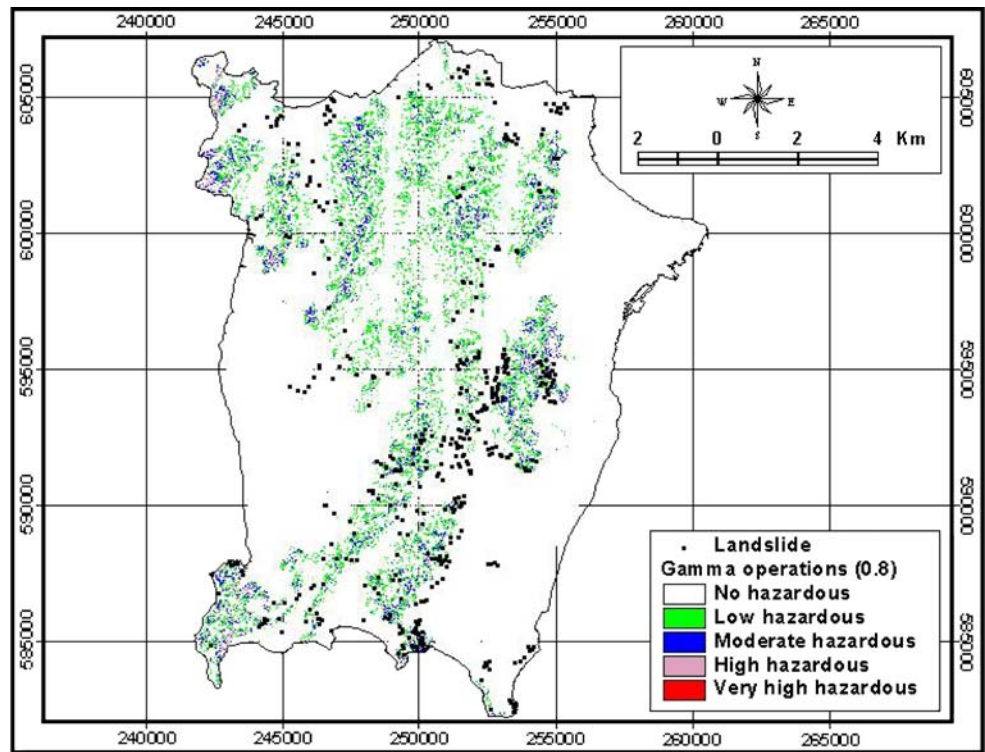


(a) Application of fuzzy algebraic “sum” operator

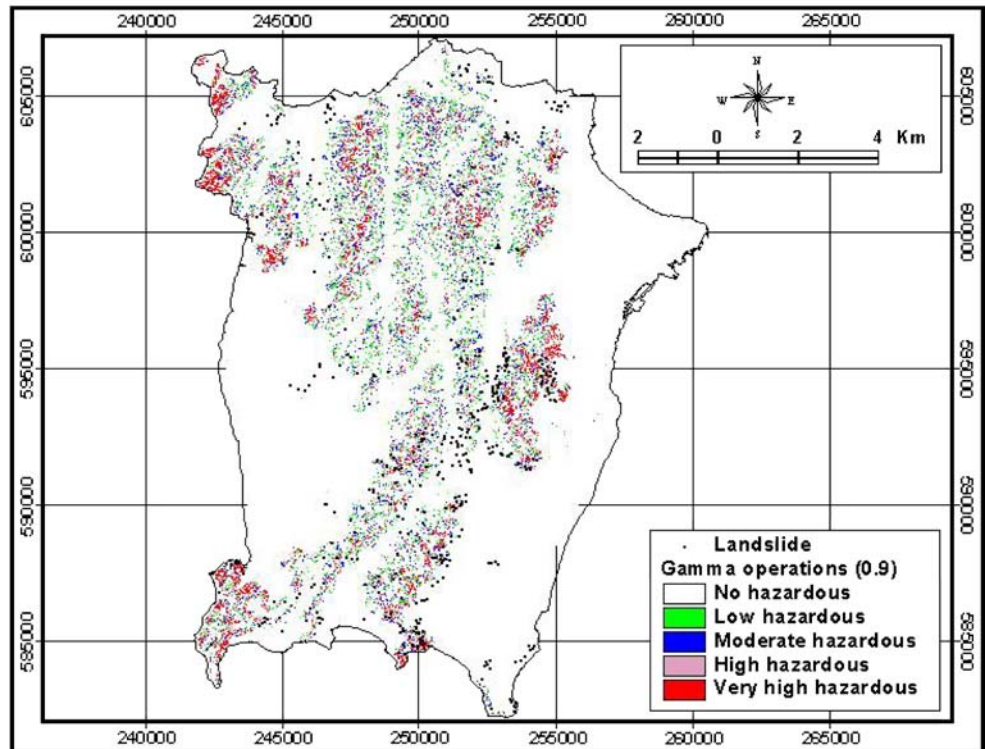


(b) Application of fuzzy algebraic “and” operator

Fig. 2 (continued)

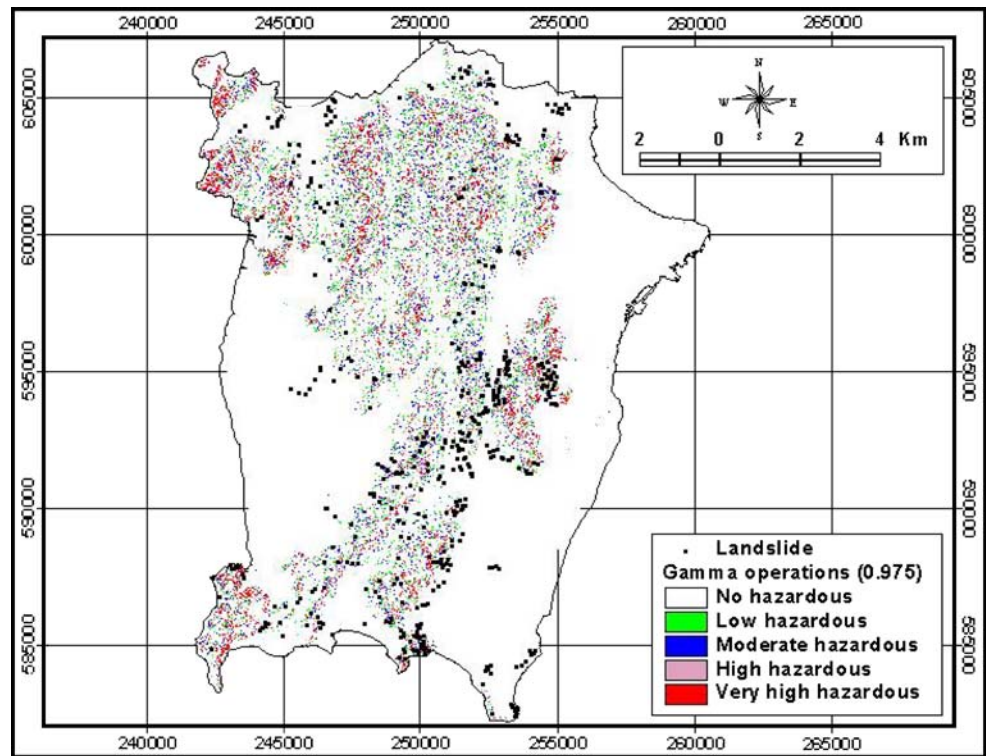


(c) Application of fuzzy gamma ($\lambda = 0.8$) operator



(d) Application of fuzzy gamma ($\lambda = 0.9$) operator

Fig. 2 (continued)



(e) Application of fuzzy gamma ($\lambda = 0.975$) operator

Verification of the fuzzy logic model and hazard maps

The landslide-hazard analysis results were verified using the existing landslide locations in the study area. The verification method was performed by comparison of existing landslide data and newly recorded landslide location data collected from field of the study area. The comparison results are shown in Fig. 3 as a line graph,

which illustrates how well the landslide-hazard maps of nine cases match with respect to the landslides used in constructing those landslide-hazard maps. To obtain the data for Fig. 3, relative ranks of landslide-hazard map and landslide occurrence were compared for each case. For this aim, the probabilities were divided into classes of accumulated area ratio % (*X*-axis) according to the landslide-hazard index value (*Y*-axis).

Fig. 3 Illustration of cumulative frequency diagram showing landslide susceptibility index rank (*X*-axis) occurring in cumulative percent of landslide occurrence (*Y*-axis)

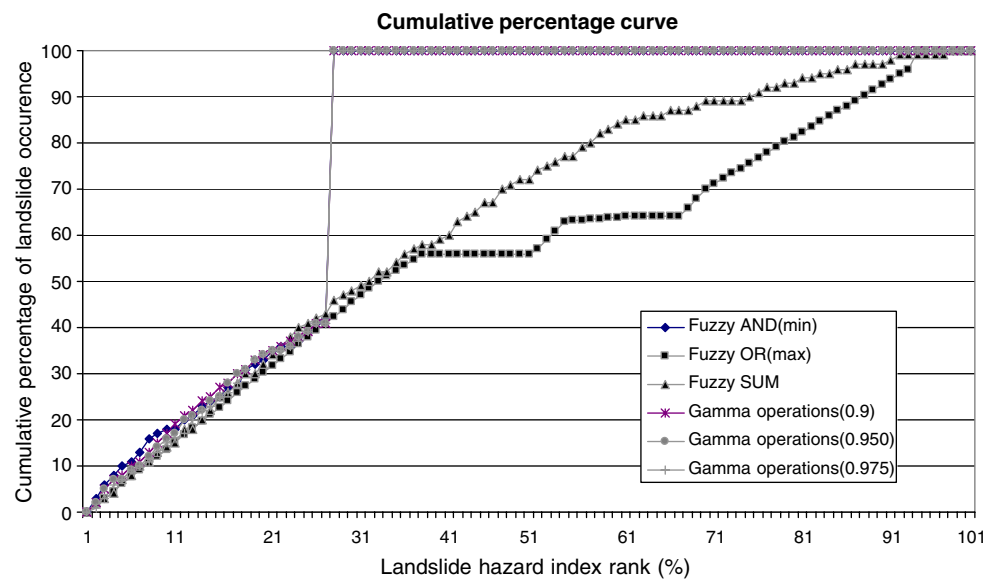


Table 3 Verification results using area under curve (AUC)

Fuzzy operator	Prediction accuracy (%)
Fuzzy and	79.49
Fuzzy or	56.86
Fuzzy algebraic sum	64.77
Fuzzy algebraic product	77.51
Gamma (λ)=0.025	79.34
Gamma (λ)=0.05	79.73
Gamma (λ)=0.1	79.73
Gamma (λ)=0.2	79.73
Gamma (λ)=0.3	79.73
Gamma (λ)=0.4	79.73
Gamma (λ)=0.5	79.73
Gamma (λ)=0.6	79.73
Gamma (λ)=0.7	79.73
Gamma (λ)=0.8	80.26
Gamma (λ)=0.9	79.49
Gamma (λ)=0.95	79.32
Gamma (λ)=0.975	79.14

For example, when applying fuzzy algebraic sum, the 90–100% (10%) class with the highest probability of a landslide contains 54% and the 80%–100% class (20%) contains 45% of the landslides of study area. In the case of applying the fuzzy and product, the 90%–100% (10%) class with the highest probability of a landslide contains 45% and the 80%–100% class (20%) contains 64% of the landslides of study area. In the case of the gamma operator ($\lambda=0.975$), the 90%–100% (10%) class with the highest possibility of a landslide contains 58% and the 80–100% class (20%) contains 68% of the landslides of study area. In the case of applying the gamma operator ($\lambda=0.8$), the 90–100% (10%) class with the highest possibility of a landslide contains 53% and 80–100% class (20%) contains 65% of the landslides of study area.

To compare the results quantitatively, the areas under the curve were recalculated taking the total area as 1, which means perfect prediction accuracy. So, the area under a curve can be used to assess the prediction accuracy qualitatively for landslide-hazard mapping. The area under the curve is shown in Table 3. For example, in the case of applying fuzzy algebraic and, the area ratio was 0.7949 and we could say that the prediction accuracy is 79.49%. In the case of applying fuzzy algebraic sum, the area ratio was 0.6477 and we could say that the prediction accuracy is 64.77%. In the case of applying the gamma operator ($\lambda=0.975$), the area ratio was 0.7914 and the prediction accuracy is 79.14%.

Discussion and conclusions

Different fuzzy operators and different λ values for the gamma operation were tested on the input fuzzy membership functions to generate the most reliable landslide-hazard map. The membership values assigned to each evidence map also play an important role in the final results. The fuzzy operators used in the first or further steps of analyses also affect the possibilities obtained in the final hazard map.

After verification, among the 17 cases, the case of applying the gamma operator ($\lambda=0.8$), showed the best accuracy (80.26%), whereas the fuzzy algebraic sum (64.77%) and fuzzy or (56.86%) operators showed the worst accuracy. In the case of applying the gamma operator with different λ value, the prediction accuracy had a similar value, between 79.14% and 80.26%. Generally, the verification results showed satisfactory agreement between the hazard map and the existing data from landslide locations. The effect of choosing different values of gamma (between 0 and 1) is not large. Because the landslide-hazard maps using different values of gamma (Fig. 2) are very similar and the prediction accuracy after verification is also very similar.

In the study, the data-derived model (frequency ratio) and the knowledge-derived model (fuzzy logic) were combined. As a result, the combined data- and knowledge-derived model is useful for landslide-hazard mapping considering the prediction accuracy. Decision-making under uncertainty is closely related to hazard analysis. Landslide-hazard map will help for decision-making for planners. These decisions are usually in the form of technical countermeasures, regulatory management or combinations of the two. Classic examples of regulatory management are zoning maps which, for instance, exclude some areas from habitation. Regulatory management is often quite intricate in prescribing different permit procedures which may include detailed evaluations and additional exploration or even go so far to prescribing particular slope designs (e.g., slope grades). The latter is actually a combination of regulatory and technical management. Technical mitigating measures range from a variety of stabilizing measures to protective measures such as rock-fall galleries to warning devices. One of the most important steps of developing a hazard-mitigation plan is assessing risks, or estimating potential losses to the people and properties within the landslide prone area.

Acknowledgments Thanks are due to the Alexander von Humboldt Foundation, Germany for awarding a guest researcher position and necessary funding to carry out the research project at Dresden University of Technology, Germany.

References

- Akgun A, Dag S, Bulut F (2007) Landslide susceptibility mapping for a landslide-prone area (Findikli, NE of Turkey) by likelihood-frequency ratio and weighted linear combination models. *Env Geol* 54(6):1127–1143
- Baeza C, Corominas J (2001) Assessment of shallow landslide susceptibility by means of multivariate statistical techniques. *Earth Surf Proc Land* 26:1251–1263
- Bonham-Carter GF (1994) Geographic information systems for geoscientists. Modelling with GIS
- Carro M, De Amicis M, Luzi L, Marzorati S (2003) The application of predictive modeling techniques to landslides induced by earthquakes: the case study of the 26 September 1997 Umbria-Marche earthquake (Italy). *Eng Geol* 69:139–159
- Catani F, Casagli N, Ermini L, Righini G, Menduni G (2005) Landslide hazard and risk mapping at catchment scale in the Arno River Basin. *Landslides* 2(4):329–343
- Cevik E, Topal T (2003) GIS-based landslide susceptibility mapping for a problematic segment of the natural gas pipeline, Hendek (Turkey). *Env Geol* 44:949–962
- Clerici A, Perego S, Tellini C, Vescovi P (2002) A procedure for landslide susceptibility zonation by the conditional analysis method. *Geomorphology* 48:349–364
- Clerici A, Perego S, Tellini C, Vescovi P (2006) A GIS-based automated procedure for landslide susceptibility mapping by the conditional analysis method: the Baganza valley case study (Italian Northern Apennines). *Env Geol* 50:941–961
- Dahal RK, Hasegawa S, Nonomura S, Yamanaka M, Masuda T, Nishino K (2007) GIS-based weights-of-evidence modelling of rainfall-induced landslides in small catchments for landslide susceptibility mapping. *Env Geol* 54(2):311–324
- Dai FC, Lee CF (2002) Landslide characteristics and slope instability modeling using GIS, Lantau Island, Hong Kong. *Geomorphology* 42:213–228
- Donati L, Turrini MC (2002) An objective method to rank the importance of the factors predisposing to landslides with the GIS methodology: application to an area of the Apennines (Valnerina; Perugia, Italy). *Eng Geol* 63:277–289
- Ercanoglu M, Gokceoglu C (2002) Assessment of landslide susceptibility for a landslide-prone area (north of Yenice, NW Turkey) by fuzzy approach. *Env Geol* 41:720–730
- Gokceoglu C, Sonmez H, Ercanoglu M (2000) Discontinuity controlled probabilistic slope failure risk maps of the Altindag (settlement) region in Turkey. *Eng Geol* 55:277–296
- Gomez HT, Kavzoglu T (2005) Assessment of shallow landslide susceptibility using artificial neural networks in Jabonosa River Basin, Venezuela. *Eng Geol* 78(1–2):11–27
- Guzzetti F, Carrara A, Cardinali M, Reichenbach P (1999) Landslide hazard evaluation: a review of current techniques and their application in a multi-scale study, Central Italy. *Geomorphology* 31:181–216
- Jibson WR, Edwin LH, John AM (2000) A method for producing digital probabilistic seismic landslide hazard maps. *Eng Geol* 58:271–289
- Lamelas MT, Marinoni O, Hoppe A, Riva J (2008) Doline probability map using logistic regression and GIS technology in the central Ebro Basin (Spain). *Env Geol* 54(5):963–977
- Lee S (2007) Application and verification of fuzzy algebraic operators to landslide susceptibility mapping. *Env Geol* 52:615–623
- Lee S, Pradhan B (2006) Probabilistic landslide risk mapping at Penang Island, Malaysia. *J Earth Syst Sci* 115(6):1–12
- Lee S, Pradhan B (2007) Landslide hazard mapping at Selangor, Malaysia using frequency ratio and logistic regression models. *Landslides* 4:33–41
- Lee S, Ryu JH, Min K, Won JS (2003a) Landslide susceptibility analysis using GIS and artificial neural network. *Earth Surf Proc Land* 27:1361–1376
- Lee S, Ryu JH, Lee MJ, Won JS (2003b) Landslide susceptibility analysis using artificial neural network at Boeun, Korea. *Env Geol* 44:820–833
- Lee S, Ryu JH, Won JS, Park HJ (2004a) Determination and application of the weights for landslide susceptibility mapping using an artificial neural network. *Eng Geol* 71:289–302
- Lee S, Choi J, Min K (2004b) Probabilistic landslide hazard mapping using GIS and remote sensing data at Boeun, Korea. *Int J Remote Sens* 25:2037–2052
- Luzi L, Pergalani F, Terlien MTJ (2000) Slope vulnerability to earthquakes at subregional scale, using probabilistic techniques and geographic information systems. *Eng Geol* 58:313–336
- Mansor S, Pradhan B, Daud M, Jamaludin N, Khuzaimah, Z (2007) Landslide susceptibility analysis using an artificial neural network Proceedings of SPIE - Volume 6749, Remote Sensing for Environmental Monitoring, GIS Applications, and Geology VII, Manfred Ehlers, Ulrich Michel, Editors 6749 J: 1–7
- Ohlmacher GC, Davis JC (2003) Using multiple logistic regression and GIS technology to predict landslide hazard in northeast Kansas, USA. *Eng Geol* 2157:1–13
- Parise M, Jibson WR (2000) A seismic landslide susceptibility rating of geologic units based on analysis of characteristics of landslides triggered by the 17 January, 1994 Northridge, California earthquake. *Eng Geol* 58:251–270
- Pistocchi A, Luzi L, Napolitano P (2002) The use of predictive modeling techniques for optimal exploitation of spatial databases: a case study in landslide hazard mapping with expert system-like methods. *Env Geol* 41:765–775
- Pradhan B, Lee S (2007) Utilization of optical remote sensing data and GIS tools for regional landslide hazard analysis by using an artificial neural network model at Selangor, Malaysia. *Earth Science Frontier* 14(6):143–152
- Pradhan B, Lee S (2008) Landslide risk analysis using artificial neural network model focusing on different training sites. *International Journal of Physical Sciences* 3(11):1–15
- Pradhan B, Singh RP, Buchroithner MF (2006) Estimation of stress and its use in evaluation of landslide prone regions using remote sensing data. *Adv Space Res* 37:698–709
- Pradhan B, Lee S, Mansor S, Buchroithner M, Jamaluddin M, Khujaimah Z (2008) Utilization of optical remote sensing data and geographic information system tools for regional landslide hazard analysis by using binomial logistic regression model. *J Appl Remote Sens* 2:1–11
- Refice A, Capolongo D (2002) Probabilistic modeling of uncertainties in earthquake-induced landslide hazard assessment. *Computer & Geosciences* 28:735–749
- Romeo R (2000) Seismically induced landslide displacements: a predictive model. *Eng Geol* 58:337–351
- Rowbotham D, Dudycha DN (1998) GIS modeling of slope stability in Phewa Tal watershed, Nepal. *Geomorphology* 26:151–170
- Shou KJ, Wang CF (2003) Analysis of the Chiufengershan landslide triggered by the 1999 Chi-Chi earthquake in Taiwan. *Eng Geol* 68:237–250
- Süzen ML, Doyuran V (2004) A comparison of the GIS based landslide susceptibility assessment methods: multivariate versus bivariate *Environmental Geology* 45:665–679
- Tangestani MH (2004) Landslide susceptibility mapping using the fuzzy gamma approach in a GIS, Kakan catchment area, southwest Iran. *Aust J Earth Sci* 51:439–450
- Tunusluoglu MC, Gokceoglu C, Nefeslioglu HA, Sonmez H (2007) Extraction of potential debris source areas by logistic regression technique: a case study from Barla, Besparmak

- and Kapi mountains (NW Taurids, Turkey). *Env Geol* 54 (1):9–22
- Wang HB, Sassa K (2005) Comparative evaluation of landslide susceptibility in Minamata area, Japan. *Env Geol* 47:956–966
- Xie M, Esaki T, Cai M (2004) A time-space based approach for mapping rainfall-induced shallow landslide hazard. *Env Geol* 46:840–850
- Zadeh LA (1965) Fuzzy sets. *Inf Control* 8:338–253
- Zhou CH, Lee CF, Li J, Xu ZW (2002) On the spatial relationship between landslides and causative factors on Lantau Island, Hong Kong. *Geomorphology* 43:197–207
- Zhou G, Esaki T, Mitani Y, Xie M, Mori J (2003) Spatial probabilistic modeling of slope failure using an integrated GIS Monte Carlo simulation approach. *Eng Geol* 68:373–386
- Zimmerman HZ (1996) *Fuzzy sets theory and its applications*. Kluwer, Dordrecht